



Fabrication and Characterization of Ternary CuAlMn Shape Memory Alloy with Novel Operation Temperatures

Canan AKSU CANBAY^{1*}, Aysegul DERE²

¹Firat University, Department of Physics, Elazig, 23200 TURKEY

Shape memory alloys (SMAs) have reached a numberless utilization in a wide range areas of modern technology over the last few decades. This is mostly because these smart materials have some very useful distinctive properties such as shape memory effect (SME), and superelasticity (SE), or damping. The most commonly preferred SMAs due to the superior SME and SE properties are the expensive NiTi alloys that constitute a majority commercial SMAs. Therefore, been regarded as the closest alternative to NiTi SMAs, the cost effective and easier processable Cu-based SMAs are focused by researchers in SMA related areas in order to improve their SMA properties by some methods. Adding one or more grain refining alloying elements (Mn, Ni) to binary Cu-based SMAs (e.g. Cu-Al) is one of such ways. One of the resultants, the ternary CuAlMn Heusler SMAs have already proved their good SMA properties and these SMAs can potentially be improved more by future research. In this work, the Cu-rich ternary CuAlMn SMA with minor amount of Mn content was fabricated by arc melting technique. After homogenizing the alloy in β -phase region and quenching it in ice-brine water to form the $\beta 1'$ martensite phase in the alloy, the SME properties were loaded in the alloy. The SME features of the produced CuAlMn SMA were studied by conducting some calorimetric and structural measurements. The differential scanning calorimetry (DSC) tests were performed to reveal the pairs of interchanging opposite-way endo/exo martensitic phase transformation peaks on the heating and cooling fragments of the DSC curves of the alloy as a sign of SME property of the alloy. The characteristic martensitic transformation temperatures and the enthalpy change values of the alloy were directly obtained by DSC peak analyses. Some other thermodynamical parameters of martensitic transformations of the alloy such as the hysteresis gap, entropy change values and equilibrium temperature were also calculated. The high temperature behavior of the CuAlMn alloy was observed by doing differential thermal analysis (DTA) measurement. The composition of the alloy (at.%) was determined by EDX test performed in room conditions. The X-ray measurement conducted at room temperature displayed and proved the successful formation of martensite structures. The results showed that the produced CuAlMn alloy has SME properties and its own martensitic transformation temperatures that can be included in the SMA properties spectrum of CuAlMn SMAs present in the literature.

Keywords: CuAlMn shape memory alloy, Martensite, Shape memory effect, Arc melting, DSC, DTA

Submission Date: 23 June 2021

Acceptance Date: 26 October 2021

*Corresponding author: caksu@firat.edu.tr

1. Introduction

Shape memory alloys (SMAs) are the alloys that can exhibit switching to their first original shapes when they are exposed to heat (or other external physical stimuli; electric, magnetic or mechanical forces) after been deformed mechanically [1]. The mechanism under such a shape changing phenomenon, named as shape memory effect (SME) behavior, is the solid solid phase transformations occur between the reversibly interchanging low temperature martensite phase (product phase) and high temperature austenite phase (parent phase) and is triggered by internal stresses which induced by the external stimuli [1, 2]. The start and finish temperatures of these two phases from the lowest to the highest are $M_f < M_s < A_s < A_f$ (in some cases M_s was found to be a bit higher than A_f) and these are called as martensitic transformation temperatures and are characteristic parameters for SMAs which have SME property. Superelasticity (SE) or pseudoelasticity (PE) is another functional property of SMAs. If SMAs with SE property are mechanically deformed by loading in a temperature range above A_f temperature, they exhibit SE behavior by recovering back to their austenite shape upon the deformer load is remove [1, 2]. Due to having such unique properties, SMAs are utilized in a very wide range of technological and industrial application areas such as medical, automotive, actuator, sensor, aviation, aerospace, textile, etc. [1-3].

The class of SMAs are mainly based on NiTi, Cu-based and Fe-based SMA systems. Among these alloy groups, the NiTi SMAs hold the most of the global SMA market share due to their superior SMA properties. However, their high costs and hard processability are their main disadvantages when compared with Cu-based SMAs which are superior to Fe-based SMAs. Although Cu-SMAs exhibit inferior SMA characteristics to NiTi ones, they are far more cheap and have better thermal and electrical conductivities [4, 5], and high damping (like CuAlMn SMAs) [3] properties. But, they have also weak mechanical properties and large grain sizes that lead brittleness in these alloys [2, 6]. Some methods are used to reduce the grain size and modify the SMA parameters such as adding one or more additive grain refining alloying elements or using different production techniques [5-10]. Hence, to improve or modify the properties of Cu-based SMAs (principally the ternary CuAlMn, CuAlNi and CuZnAl SMAs) is an attractive research subject for the related researchers. Among Cu-based SMAs, CuAlMn SMAs has great interest for their good ductility, strain recovery and superelasticity (or damping) features [6, 8, 11]. These promising alloys are tried to modified and improved more, for example different high transformation

temperatures (or operating temperature ranges) with improved SMA properties, which are demanded in some industrial areas like automotive [12].

In this experimental work, an arc melted CuAlMn shape memory alloy was investigated by some thermal and structural SME characterization tests to uncover its transformation temperatures and some SME characteristics.

2. Experimental

The ternary 71.56Cu-25.36Al-3.08Mn at.% or (84.20Cu-12.67Al-3.13Mn wt.%) shape memory alloy was prepared from powders of high purity (99.9%) copper, aluminum, and manganese elements. In the beginning of the alloy's fabrication process, the element powders weighed on a precision balance were mixed, then the mixture was pelletized under pressure. Then these pellets together were melted by an induction melter under inert argon atmosphere and the alloy was formed as-cast ingot. Then, this ingot alloy was cut into the miniscule sized (~40-50 mg) samples proper for tests. To form the martensite structure in the alloy texture, the alloy samples were heated up and quenched from high β -phase temperature region into water. The chemical composition of the alloy was identified by taking EDX (energy dispersive X-ray) test via using a Zeiss Evo MA10 model EDX instrument in room conditions. The differential scanning calorimetry (DSC) measurements were performed at different heating/cooling rates of 15, 20, 25, 30 and 35 °C/min to determine the characteristic martensitic transformation (working) temperatures of the alloy by using a Shimadzu DSC-60A model DSC equipment with a constant flow (100 ml/min) of argon gas. The thermal behavior of the alloy in high temperature region was measured by using a Shimadzu DTG-60AH model differential thermal analysis (DTA) instrument that was run from room temperature to 900 °C at a single heating rate of 25 °C/min under the same argon gas flow. The X-ray diffraction measurement (using $\text{CuK}\alpha$ radiation) was performed by using a Rigaku RadB-DMAX II diffractometer to obtain the diffraction peaks of atomic planes of the martensite structures at room temperature.

3. Results and Discussion

The DSC curves of the CuAlMn SMA cycled at varying heating/cooling rates of 15, 20, 25, 30, and 35 °C/min are presented in Fig.1. As seen on the all down-heating fragments of these DSC curves, all of the endothermic bottom peaks that appeared at between ~80-115 °C denote the occurrences of the forward martensitic transformations from martensite (M) to austenite (A) phase; M→A. Inversely, on cooling processes of the alloy, the peaks seen

up at between ~40-51 °C refer to the correspondent back exothermic austenite to martensite (A→M) transformations. The characteristic martensitic transformation temperatures (A_s , A_f , M_s , and M_f) and the values of some other kinetic parameters; A_{max} , hysteresis gap (A_s - M_f difference), T_0 (thermal equilibrium temperature), and enthalpy (ΔH) and entropy (ΔS) change amounts (for $M \rightarrow A$ transitions) that were determined by making DSC peak analyses and the results of the related computations were all tabulated in Table 1.

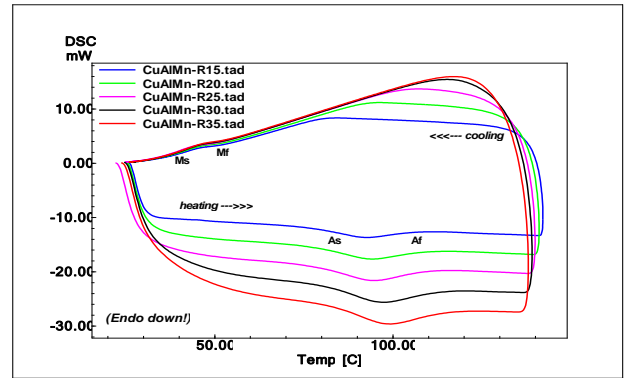


Fig.1. The DSC curves of the produced CuAlMn SMA at different heating/cooling rates

Table-1: The martensitic transformation temperatures and thermodynamical parameters of the CuAlMn shape memory alloy

Heating/cooling rate (°C/min)	A_s (°C)	A_f (°C)	A_{max} (°C)	M_s (°C)	M_f (°C)	A_s - M_f (°C)	T_0 (°C)	$\Delta H_{M \rightarrow A}$ (J/g)	$\Delta S_{M \rightarrow A}$ (J/g°C)
15	79.20	106.48	92.73	50.19	41.90	37.30	78.335	3.09	0.0394
20	78.14	109.96	94.17	50.69	41.19	36.95	80.325	3.59	0.0447
25	77.90	110.56	94.96	49.40	40.49	37.41	79.98	3.69	0.0460
30	80.90	113.88	97.33	50.80	42.39	38.51	82.34	3.46	0.0420
35	83.06	115.37	99.46	51.01	43.37	37.30	78.335	3.44	0.0390

The thermodynamic equilibrium temperature (T_0) is the temperature at where the magnitudes of Gibbs free energy (G) amounts of the interchangeable austenite and martensite phases are equalized. The T_0 values of the CuAlMn alloy for each heating/cooling rate were found by using $T_0 = (A_f + M_s)/2$ formula [4, 5]. Then, by substituting these T_0 values in $\Delta S_{M \rightarrow A} = \Delta H_{M \rightarrow A} / T_0$ relation [4, 5] the entropy change ($\Delta S_{M \rightarrow A}$) values for the endothermic $M \rightarrow A$ transitions at each heating rate were found.

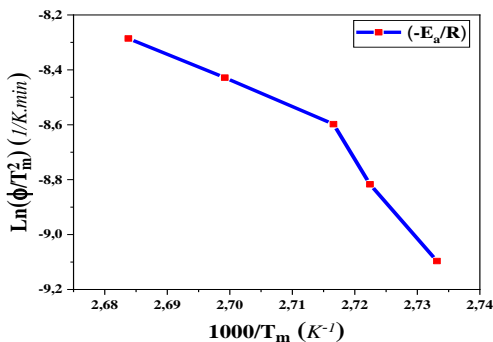


Fig.2. Activation energy change graphic

The activation energy (E_a) parameter of SMAs is also an important thermodynamic parameter which is an energy

barrier level that must be overcome for a martensitic transformation to occur and it depends on heating rate.

This energy barrier determines the crystallization behavior of the alloys. The value of the activation energy barrier for the CuAlMn SMA can be found from the peak shifts in the DSC curves run at different heating rates by using the Kissinger formula [4, 13] given below;

$$\frac{d[\ln(\Phi/T_m^2)]}{d(1/T_m)} = -\frac{E_a}{R} \quad (1)$$

where; Φ stands for heating/cooling rate, T_m refers to peak temperature (A_{max}) of endothermic $M \rightarrow A$ transformation, and R is the universal gas constant ($R = 8.314 \text{ J/mol.K}$). A plot of $\ln(\Phi/T_m^2)$ versus $1000/T_m$ (presented in Fig.2) showing how the activation energy (E_a) changes by heating rate was drawn to find the term on the left side of Eq.1 which is equal to the linear fitting slope value of this plot. By applying linear fit on this activation energy change plot, the slope value was obtained, and then substituting this value as the left term in the Eq.1, the E_a activation energy barrier of the alloy was found as 130.46 kJ/mol.

The DTA heating curve of the CuAlMn SMA taken at the single DTA heating rate of 25 °C/min is given in Fig.3. The humps down and up peaks that appear on this heating curve along from far-left to the right-end indicate the multiple

phase transitions array of $\beta 1' \rightarrow \beta 1(L2_1) \rightarrow B2 \rightarrow \alpha$ and $\gamma 2$ precipitating (388-507 °C) \rightarrow eutectoid reversion (~ 521 °C) $\rightarrow B2 \rightarrow A2$, which is a common phase transformation array to the Cu-Al based SMAs [5,14-18].

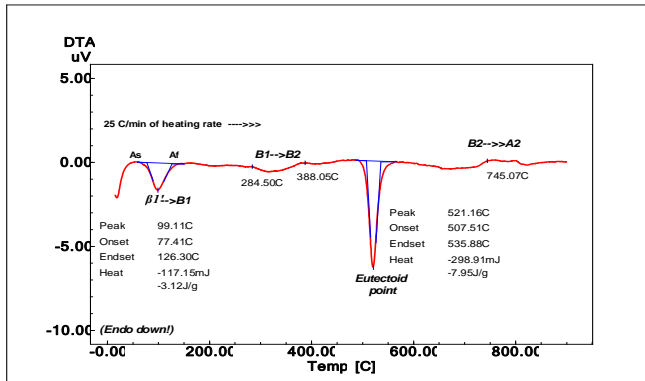


Fig.3. The DTA heating curve of the CuAlMn SMA that was obtained at the single heating rate of 25 °C/min. The humps down and up peaks that appear on this heating curve along from far-left to the right-end indicate the multiple phase conversion array of $\beta 1' \rightarrow \beta 1(L2_1) \rightarrow B2 \rightarrow$ precipitating (388-507 °C) \rightarrow eutectoid reversion (~ 521 °C) $\rightarrow B2 \rightarrow A2$, a common behavior of the Cu-Al based SMAs generally observed during the processes of heating these alloys up to high β -phase region

To calculate the value of the average valence electron concentration per atom (e/a) parameter for a Cu-based SMA can give us some clues about the presence of the martensite phases formed within relative volumes in that alloy. The e/a parameter strongly affects on the entropy change of average periodic lattice formation. The e/a value of the fabricated CuAlMn SMA can be calculated by using $e/a = \sum f_i v_i$ formula [5, 14], where f_i refers to the atomic fractions (at.%) of the alloying elements and v_i is the corresponding valence electron values of these elements. Thus, the e/a value was found as 1.538, which is above the critical e/a value range of 1.45-1.49 and therefore presages that the hexagonal $\gamma 1'(2H)$ type martensite must have been formed as the dominant martensite phase together with the secondary monoclinical $\beta 1'(M18R)$ type martensite phase in the alloy [5, 14-16]. This assesment deduced from the e/a value of the alloy is discussed in the following section of X-ray diffraction test results.

The XRD pattern obtained by diffracting $CuK\alpha$ waves from the CuAlMn alloy is given in Fig.4. The observed peaks all belong to the martensite phases, the highest peak is monoclinical $\beta 1'(0022)$ at the bragg angle of 42.87° and the other peaks are $\beta 1'(122)$, $\beta 1'(128)$, $\beta 1'(1210)$, $\beta 1'(2012)$, $\beta 1'(040)$, $\beta 1'(042)$, and the hexagonal $\gamma 1'(020)$, $\gamma 1'(202)$, $\gamma 1'(002)$, $\gamma 1'(012)$, $\gamma 1'(211)$, $\gamma 1'(212)$, $\gamma 1'(221)$ [5, 19-26]. As seen, both of the $\beta 1'$ and $\gamma 1'$ martensites co-exist in the CuAlMn alloy matrix, as expected in the e/a

assesment. The XRD result also showed that the alloy has a polycrystalline structure. The crystallite size of the alloy can be found by using $D = 0.9\lambda/B_{1/2}\cos\theta$ formula of Debye-Scherrer [15, 20], where λ is the used X-ray wavelength of the $CuK\alpha$ radiation ($\lambda = 0.15406$ nm), $B_{1/2}$ is full width at half maximum (FWHM) value (0.38°) of the highest peak, and θ is Bragg angle of the diffraction. Thus, the average crystallite size (D) value of the CuAlMn alloy was calculated as 22.46 nm.

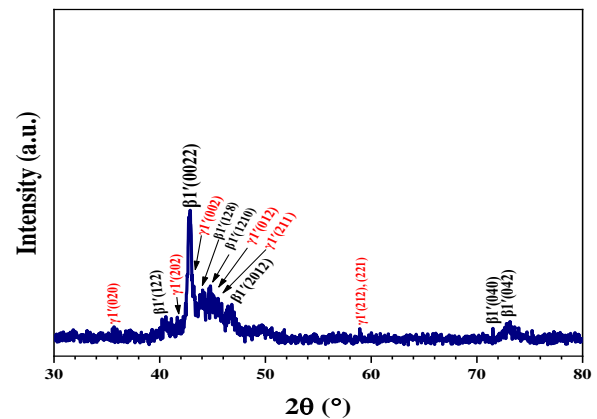


Fig.4. The X-ray diffraction pattern of CuAlMn SMA

4. Conclusion

The CuAlMn was successfully produced by induction melting method and thermal and structural SME characteristics of the alloy were uncovered. The novel characteristic martensitic transformation temperature range (operation temperature range) of this SMA is observed to be as ~ 40 - 115 °C. The structure of the alloy was demonstrated to be polycrystalline nature including both types of the 18R and 2H martensite phases at room temperature. The obtained results shows that this CuAlMn can be used in various applications.

References

- [1] K. Otsuka , C. Wayman, Shape Memory Materials, Cambridge University Press, 1998, pp.xiii-5.
- [2] Jaronie Mohd Jani, Martin Leary, Aleksandar Subic, Mark A. Gibson, A review of shape memory alloy research, applications and opportunities, Materials & Design (1980-2015), Vol. **56**, 2014, Pages 1078-1113, <https://doi.org/10.1016/j.matdes.2013.11.084>
- [3] D.C. Lagoudas (Ed.). *Shape Memory Alloys: Modeling and Engineering Applications*. Springer Science+Business Media LLC, New York (2008).
- [4] Canbay, C.A., Karaduman, O. & Özkul, İ. Lagging temperature problem in DTA/DSC measurement on

- investigation of NiTi SMA. *J Mater Sci: Mater Electron* **31**, 13284–13291 (2020). <https://doi.org/10.1007/s10854-020-03881-y>
- [5] Canbay, C. A., & Karaduman, O. (2021). The photo response properties of shape memory alloy thin film based photodiode. *Journal of Molecular Structure*, **1235**, 130263. <https://doi.org/10.1016/j.molstruc.2021.130263>
- [6] Yang, J., Wang, Q. Z., Yin, F. X., Cui, C. X., Ji, P. G., & Li, B. (2016). Effects of grain refinement on the structure and properties of a CuAlMn shape memory alloy. *Materials Science and Engineering: A*, **664**, 215-220. <https://doi.org/10.1016/j.msea.2016.04.009>
- [7] Zhang, X., & Liu, Q. S. (2016). Influence of alloying element addition on Cu–Al–Ni high-temperature shape memory alloy without second phase formation. *Acta Metallurgica Sinica (English Letters)*, **29**(9), 884-888. <https://doi.org/10.1007/s40195-016-0467-1>
- [8] U.S. Mallik, V. Sampath (2008). Influence of quaternary alloying additions on transformation temperatures and shape memory properties of Cu–Al–Mn shape memory alloy. *Journal of Alloys and Compounds* **469** (2009) 156–163. <https://doi.org/10.1016/j.jallcom.2008.01.128>
- [9] Özkul, İ., Kurgun, M. A., Kalay, E., Canbay, C. A., & Aldaş, K. (2019). Shape memory alloys phenomena: classification of the shape memory alloys production techniques and application fields. *The European Physical Journal Plus*, **134**(12), 585. <https://doi.org/10.1140/epjp/i2019-12925-2>
- [10] López Cuellar, Enrique, López Pavón, Luis, Nuñez Mendoza, Esaú, Araújo, Carlos José De, Castro, Walman Benicio De, Gonzalez, Cezar, & Otubo, Jorge. (2016). Effect of Spun Velocities and Composition on the Microstructure and Transformation Temperatures of TiNi Shape Memory Ribbons. *Materials Research*, **19**(5), 1132-1137. Epub September 12, 2016. <https://doi.org/10.1590/1980-5373-MR-2015-0380>
- [11] Babacan, N., Pauly, S., & Gustmann, T. (2021). Laser powder bed fusion of a superelastic Cu-Al-Mn shape memory alloy. *Materials & Design*, **203**, 109625. <https://doi.org/10.1016/j.matdes.2021.109625>
- [12] Mohd Jani, J., Leary, M., & Subic, A. (2017). Designing shape memory alloy linear actuators: A review. *Journal of Intelligent Material Systems and Structures*, **28**(13), 1699-1718. <https://doi.org/10.1177/1045389X16679296>
- [13] Kissinger, H. E. (1957). Reaction kinetics in differential thermal analysis. *Analytical chemistry*, **29**(11), 1702-1706. <https://doi.org/10.1021/ac60131a045>
- [14] O. Karaduman et al., Analysis of a newly composed Cu-Al-Mn SMA showing acute SME characteristics. *AIP Conference Proceedings* **2178**, 030039 (2019). <https://doi.org/10.1063/1.5135437>
- [15] C.A. Canbay, et al., Heat treatment and quenching media effects on the thermodynamical, thermoelastical and structural characteristics of a new Cu-based quaternary shape memory alloy, *Compos. Part B* **174** (2019) 106940. <https://doi.org/10.1016/j.compositesb.2019.106940>
- [16] Canbay, C. A., Karaduman, O., Özkul, I., & Ünlü, N. (2020). Modifying Thermal and Structural Characteristics of CuAlFeMn Shape Memory Alloy and a Hypothetical Analysis to Optimize Surface-Diffusion Annealing Temperature. *Journal of Materials Engineering and Performance*, **29**(12), 7993-8005. <https://doi.org/10.1007/s11665-020-05241-7>
- [17] Prado, M.O., et al. (1995), “Martensitic transformation in Cu-Mn-Al alloys”, *Scripta Metallurgica et Materialia*, **33**(6), 877–883. [https://doi.org/10.1016/0956-716X\(95\)00292-4](https://doi.org/10.1016/0956-716X(95)00292-4)
- [18] S.M. Chentouf, et al., (2009). Microstructural and thermodynamic study of hypoeutectoidal Cu–Al–Ni shape memory alloys. *Journal of Alloys and Compounds*, **470**: pp.507–514. <https://doi.org/10.1016/j.jallcom.2008.03.009>
- [19] Canbay, C. A., Karaduman, O., & Özkul, İ. (2019). Investigation of varied quenching media effects on the thermodynamical and structural features of a thermally aged CuAlFeMn HTSMA. *Physica B: Condensed Matter*, **557**, 117-125. <https://doi.org/10.1016/j.physb.2019.01.011>
- [20] Canbay, C. A., Karaduman, O., Ünlü, N., Özkul, İ., & Çiçek, M. A. (2021). Energetic Behavior Study in Phase Transformations of High Temperature Cu–Al–X (X: Mn, Te, Sn, Hf) Shape Memory Alloys. *Transactions of the Indian Institute of Metals*, 1-12. <https://doi.org/10.1007/s12666-021-02241-6>
- [21] Xiao, Z., Fang, M., Li, Z., Xiao, T., & Lei, Q. (2014). Structure and properties of ductile CuAlMn shape memory alloy synthesized by mechanical alloying and powder metallurgy. *Materials & Design*, **58**, 451-456. <https://doi.org/10.1016/j.matdes.2014.02.029>
- [22] Karaduman, O., Canbay, C. A., Ünlü, N., & Özkul, İ. (2019, November). Analysis of a newly composed Cu-Al-Mn SMA showing acute SME characteristics. In *AIP Conference Proceedings*, Vol. **2178**, No. 1, p. 030039. AIP Publishing LLC. <https://doi.org/10.1063/1.5135437>

- [23] Canbay, C. A., Karaduman, O., Ibrahim, P. A., & Özkul, İ. (2021). Thermostructural shape memory effect observations of ductile Cu-Al-Mn smart alloy. *Advances in Materials Research*, **10**(1), 45. <http://dx.doi.org/10.12989/amr.2021.10.1.045>
- [24] Canbay, C.A., Genc, Z.K. & Sekerci, M. Thermal and structural characterization of Cu–Al–Mn–X (Ti, Ni) shape memory alloys. *Appl. Phys. A* **115**, 371–377 (2014). <https://doi.org/10.1007/s00339-014-8383-6>
- [25] Canbay, C. A., Karagoz, Z., & Yakuphanoglu, F. (2014). Controlling of transformation temperatures of Cu-Al-Mn shape memory alloys by chemical composition. *Acta Physica Polonica A*, **125**(5), 1163. <https://doi:10.12693/APhysPolA.125.1163>
- [26] Yang, S., Zhang, F., Wu, J. et al. Microstructure characterization, stress–strain behavior, superelasticity and shape memory effect of Cu–Al–Mn–Cr shape memory alloys. *J Mater Sci* **52**, 5917–5927 (2017). <https://doi.org/10.1007/s10853-017-0827-x>